

Transformations between the theoretical and observational planes in the HST–NICMOS and WFPC2 photometric systems

Livia Origlia
Osservatorio Astronomico di Bologna, Via Ranzani 1, I-40127 Bologna, Italy
e-mail: origlia@astbo3.bo.astro.it

and

Claus Leitherer
Space Telescope Science Institute, 3700 San Martin Drive, Baltimore, MD 21218
e-mail: leitherer@stsci.edu

ABSTRACT

Color–temperature relations and bolometric corrections in the HST–NICMOS F1110W, F160W and F222M and in the WFPC2 F439W, F555W and F814W photometric systems, using two different sets of model atmospheres, have been derived. This database of homogeneous, self–consistent transformations between the theoretical and observational planes also allows combinations of visual and infrared quantities, without any further transformation between the two different photometric systems. The behavior of the inferred quantities with varying the stellar parameters, the adopted model atmospheres and the instrumental configurations are investigated. Suitable relations to transform colors and bolometric corrections from HST to ground–based photometric systems are also provided.

Subject headings: methods: data analysis — techniques: photometric — atlases — stars: atmospheres — stars: fundamental parameters

1. Introduction

Transformations between the theoretical and the observational planes are fundamental tools to compare stellar evolution models with observed color–magnitude diagrams. In order to calibrate suitable relations among colors, temperatures and bolometric corrections (BCs) several basic ingredients are needed:

- homogeneous and complete grids of stellar spectra (observed and/or theoretical);
- accurate filter profiles;
- reference spectra (the Sun, Vega etc.) to set the zero points of the relations;
- suitable routines to interpolate within the grids and to integrate along the spectra.

These calibrations are certainly model dependent and systematic shifts between different scales are common features. The goal of this paper is to obtain color–temperature relations and BCs in the HST–NICMOS photometric system. We also derive analogous transformations for a few selected filters in the WFPC2 system to provide homogeneous, self–consistent color–temperature relations and BCs when combinations of optical–infrared colors are used. A more complete calibration of the color–temperature transformations in the WFPC2 system can be found in the paper by Holtzman et al. (1995, hereafter H95).

In Sect. 2 we describe the code we used to derive the transformations. In Sect. 3 and 4 we discuss the transformations in the HST–NICMOS and the WFPC2 systems, respectively. In Sect. 5 we derive suitable relations to transform a few selected colors and BCs from the HST to the ground–based photometric system. In Sect. 6 we draw our conclusions.

2. The code

The synthetic colors and BCs were computed using a modified version of the evolutionary synthesis code by Leitherer et al. (1999).

We implemented two different set of model atmospheres: *i*) the compilation by Lejeune, Cuisinier & Buser (1997, hereafter LCB97), based on the ATLAS code by Kurucz and corrected to match empirical color–temperature calibrations; *ii*) the compilation by Bessell, Castelli & Plez (1998, hereafter BCP98) using only the homogeneous set of models without overshooting computed by Castelli (1997) and based on Kurucz’s ATLAS9 models. The grid of stellar parameters explored by our computations is:

- Metallicities in the range 0.01 – 1.00 solar.
- Effective temperatures T_{eff} in the range 3500 – 50000 K.
- Gravities $\log g$ in the range 0.0 – 5.0.

The ground–based BVIJHK filter profiles are in the Johnson’s (1966) photometric system and were taken from Buser & Kurucz (1978) (BV filters) and from Bruzual (1983) (IJHK filters) (see also Sect. 5 in Leitherer & Heckman 1995 for more details). The selected broadband filters in the HST–WFPC2 and NICMOS photometric systems are: F439W, F555W, F814W and F110W, F160W, F222M, respectively. The filter profiles have been multiplied by the wavelength dependent detector quantum efficiency of the four WFPC2 and the three NICMOS cameras. We used the most updated post–launch throughput curves and CCD quantum efficiencies, according to the WFPC2 and NICMOS documentation on the WEB. The quoted NICMOS throughput curves are already empirically adjusted to match standard star measurements (the correction factors are less than 10% in the case of the F110W and F160W filters and about 25% for the F222M one). We do not apply any further empirical adjustment to these response curves.

The colors have been normalized assuming 0.00 values in all passbands for a Vega–like star with $T_{\text{eff}}=9500\text{K}$, $\log g=4.0$ and $[\text{Fe}/\text{H}]=-0.5$ (cf. e.g. BCP98). The BCs have been normalized assuming a value of -0.07 for a Sun–like star with $T_{\text{eff}}=5750\text{K}$, $\log g=4.5$ and $[\text{Fe}/\text{H}]=0.0$ (cf. e.g. Montegriffo et al. 1998). Different assumptions for the colors and bolometric corrections of

Vega and Sun –like stars can be accounted for by simply scaling the inferred quantities by the corresponding amounts.

In order to quantify the influence of the adopted filter response curves on the inferred colors we also compare our B–V and V–K values with those in Table 2 of BCP98 for solar metallicity. The adopted model atmospheres are exactly the same and also similar within 0.01 mag are the reference colors for the Vega–like star. The only difference between the two sets of transformations are the adopted filter response curves. Within 0.01 mag our V–K color is fully consistent with BCP98 values, while only below 5000K our B–V becomes progressively bluer (at most 0.03 mag at 3500K).

For each model atmosphere at a given T_{eff} and $\log g$ we tabulate the corresponding colors in the form (V-F), where F is the selected filter in the ground–based or in the HST system, and the bolometric correction BC_V in the V passband. We also provided analogous colors and BCs using simple blackbodies at a given temperature.

All the tables with the computed transformations can be retrieved from <http://www.stsci.edu/science/starburs>

In the following we analyze the behavior of the inferred quantities varying the stellar parameters and the adopted model atmospheres.

3. The HST–NICMOS infrared plane

In Fig. 1 we plot the (F110W–F160W) and (F110W–F222M) color–temperature transformations in the HST–NIC2 system, using the BCP98 models for three gravities ($\log g$ of 0.0, 2.0 and 4.0) and two metallicities ($Z = Z_{\odot}$ and $Z = 0.1Z_{\odot}$). For temperatures hotter than 4000 K these infrared colors show a scatter within 0.1 mag with varying $\log g$ and Z . At lower temperatures the scatter among models with different gravities increases up to a few tenths of mag at $T_{\text{eff}}=3500$ K, while the metallicity dependence is less critical.

Pure blackbodies have systematically bluer colors than model atmospheres, especially at the coolest temperatures, as expected from the omission of molecular opacities. This means that for a given color, blackbodies are cooler than the model atmospheres.

Analogous color–temperature relations using the LCB97 models have been obtained. In Fig. 2 we report the difference of the color–temperature transformations in the NIC2 system, by adopting the BCP98 or the LCB97 model atmospheres. At temperatures below ~ 5000 K the infrared colors using the LCB97 models get progressively bluer (up to 0.2–0.3 mag) than those using the BCP98 models. This behavior mainly reflects the difference between the original and corrected grids of model atmospheres by LCB97. Comparing their Figs. 6,7 (the original synthetic colors for giants and dwarfs, respectively) with their Figs. 14,15 (the corresponding corrected models to match empirical color–temperature relations) one can see that in the range of temperatures between 4000 and 3500 K the *corrected* (J–H) ground based color is bluer (from 0.1 up to 0.3 mag) than the corresponding original value, regardless the stellar gravity. A similar comparison can be done between the original and the *corrected* (J–K) ground based color: the latter becomes bluer with decreasing temperature by about 0.2 and up to 0.3 mag for giants and dwarfs at $T_{\text{eff}}=3500$ K, respectively.

The un–corrected LCB97 models, from the original grids of atmosphere spectra by Kurucz,

should provide colors more similar to those obtained from the BCP98 models.

Color–temperature transformations in the NIC1 and NIC3 systems are also provided, as shown in Fig. 3. Regardless the model atmosphere used and the adopted stellar parameters, for a given temperature the (F110W–F160W) color in the NIC1 system is only ≤ 0.01 mag redder than in the NIC2 system, while both the (F110W–F160W) and the (F110W–F222M) colors in the NIC3 system are slightly redder (≤ 0.03 mag below ~ 4000 K).

In Fig. 4 we plot the BC in the NIC2 F110W, F160W and F222M passbands as a function of the temperature using the BCP98 models. Increasing the temperature of the stellar atmospheres, progressively larger corrections (that is smaller values of the BC) to the infrared fluxes have to be applied in order to get the bolometric luminosity. The scatter in the inferred quantities for different gravities and metallicities is generally small. At low temperatures the use of pure blackbodies requires larger corrections than using model atmospheres, as expected since the former have bluer spectra than the latter.

In Fig. 5 we plot the difference between the values of the BC in the NIC2 photometric system, adopting the BCP98 or the LCB97 models, as we did for the colors in Fig. 2. At temperatures below 5000 K, larger BC values in the F110W and F222M and smaller ones in the F160W passbands (up to ≤ 0.2 mag at $T_{\text{eff}}=3500$ K) are required when LCB97 models are used compared to the BCP98 ones.

The above trends are almost independent of the adopted metallicity.

For a given set of model atmospheres, very similar BCs within < 0.01 mag are also obtained in the NIC1 and NIC3 systems, as shown in Fig. 6. Only in the F110W passband we find that the BC values in the NIC3 system are slightly smaller (≤ 0.02 mag) than in the NIC2 system.

Our discussion on the behavior of the inferred colors and bolometric corrections with varying the stellar parameters has been limited to the low temperature domain ($T_{\text{eff}} < 5000$ K) where they are more sensitive. At higher temperatures these infrared quantities become progressively less dependent on the adopted model atmospheres.

4. The HST–WFPC2 visual plane

In Fig. 7 we plot the (F439W–F555W) and (F555W–F814W) color–temperature transformations in the HST–PC1 system, using the BCP98 models for the three gravities and two metallicities of Fig. 1.

The scatter among models with different $\log g$ and Z is ≤ 0.1 mag at all temperatures in the case of the (F555W–F814W) color, while at low temperatures ($T_{\text{eff}} \leq 5000$ K) the scatter among models with different gravities in the (F439W–F555W) color increases up to about 0.6 mag at $T_{\text{eff}}=3500$ K, while the metallicity dependence is less critical. As we found for the infrared colors, pure blackbodies show bluer colors than model atmospheres.

Analogous color–temperature relations using the LCB97 models are also obtained. In Fig. 8 we report the difference in the color–temperature transformations by adopting the BCP98 or the LCB97 model atmospheres. Using the LCB97 models, at low temperatures the (F439W–F555W) color becomes progressively bluer (up to 0.1–0.2 mag) at low gravities and only slightly redder at larger ones, compared to the values obtained from the BCP98 models. The (F555W–F814W)

color becomes rapidly redder (particularly at low gravities) than the corresponding quantities using the BCP98 models for $T_{\text{eff}} \leq 4000$ K. This behavior has little metallicity dependence. As for the infrared colors, this behavior can be mainly ascribed to the corrections applied by LCB97 to the original model atmospheres. Comparing again their Figs. 6,7 (the original synthetic colors) with their Figs. 14,15 (the corresponding corrected models) one can see that below 4000 K the *corrected* ground-based (B–V) color of giants becomes bluer and slightly redder for dwarfs, while the ground-based (V–I) color becomes rapidly redder (a few tenths of mag, even larger values for giants).

In Fig. 9 we plot the BC in the F439W, F555W and F814W passbands as a function of the temperature using the BCP98 models. The required BC values using pure blackbodies are on average slightly larger than using model atmospheres, as expected since the former have bluer spectra than the latter and, contrary to the infrared case, in the visual range they tend to be brighter than the model atmospheres.

In Fig. 10 we plot the difference between the values of the BC, adopting the BCP98 or the LCB97 models, as we did in Fig. 8 for colors. At temperatures below 5000 K, smaller BC values in the F439W and F555W and larger (up to ≤ 0.2 mag at $T_{\text{eff}}=3500$ K) in the F814W passbands are inferred if the LCB97 models are used. As for the infrared plane, the above trends are sensitive to the adopted gravity and almost independent of metallicity.

For a given set of model atmospheres, very similar color–temperature transformations and BC (within 0.01 mag) are obtained in all four WFPC2 cameras.

5. Discussion

Model atmospheres are a powerful tool to calibrate suitable color–temperature transformations since homogeneous and complete grids for a wide range of stellar parameters are available. Nevertheless, for some specific applications empirical scales even if they are less complete in terms of stellar parameters are preferred.

Using the BCP98 model atmospheres, we calibrated average relations to transform several representative colors and BCs from the HST to the ground-based photometric system where most of the empirical scales are calibrated (cf. Montegriffo et al. 1998 and references therein). All the BCP98 models included in our grid of stellar parameters for all the three NICMOS and four WFPC2 cameras have been used to compute the best fits. Very similar best fit relations can be obtained using the LCB97 model atmospheres.

In Fig. 11 the best model fits to the difference between the ground-based (J–H) and (J–K) colors and the NICMOS (F110W–F160W) and (F110W–F222M) ones, respectively, as a function of the NICMOS quantities are shown.

The derived transformations are practically metallicity and gravity independent and very similar relations can be obtained adopting a particular metallicity or gravity.

A cubic polynomial relation is required to transform the (F110W–F160W) into the ground-based (J–H) color, while a simple linear relation allows one to transform (F110W–F222M) into the ground-based (J–K) color. Very small (< 0.01 mag) global *r.m.s* values have been obtained. The maximum scatter between the best fit and the model atmospheres occurs at the lowest temperatures ($T_{\text{eff}}=3500\text{--}4000$ K) and is ≤ 0.06 mag in both colors.

For comparison, we also plot the colors of the standard stars with measured F110W, F160W and F222M and ground-based JHK magnitudes, according to the NICMOS Photometry Update WEB page (November 25, 1998), even though the quoted values are still in the process of being updated, and of a set of red stars in the Baade's window measured by Stephens et al. (1999).

Unfortunately, most of these stars are cooler than 3500K, that is out of the temperature range covered by the selected set of model atmospheres. Nevertheless, the observed quantities are reasonably reproduced (within ~ 0.1 mag) by the best model fits in the temperature range covered by the models, that is $T_{\text{eff}} \geq 3500$ K, while at lower temperatures the scatter is larger and also depends on the adopted extrapolation.

In Fig. 12 we show the best model fits to the difference between the ground-based BC_J and BC_K and the corresponding NICMOS BC_{F110W} and BC_{F222M} values, as a function of the (F110W–F160W) and (F110W–F222M) NICMOS colors, respectively. Cubic polynomial relations with even smaller scatters than for colors are required to transform the BC from the NICMOS into the ground-based infrared photometric system.

The numerical relations to transform the selected colors and BCs from the NICMOS to the ground-based photometric system are listed below:

$$(J-H) = -0.063(F110W - F160W)^3 + 0.172(F110W - F160W)^2 + 0.563(F110W - F160W) + 0.007$$

$$(J-K) = 0.803(F110W - F222M) + 0.003$$

$$BC_J = BC_{F110W} + 0.069(F110W - F160W)^3 - 0.181(F110W - F160W)^2 + 0.443(F110W - F160W) - 0.008$$

$$BC_K = BC_{F222M} + 0.023(F110W - F222M)^3 - 0.110(F110W - F222M)^2 + 0.204(F110W - F222M) - 0.001$$

In Fig. 13 the best model fits to the difference between the ground-based (B–V) and (V–I) colors and the corresponding WFPC2 (F439W–F555W) and (F555W–F814W) values as a function of the corresponding WFPC2 quantities are shown. Cubic polynomial relations are required to transform the (F439W–F555W) and the (F555W–F814W) colors into the corresponding ground-based (B–V) and (V–I) quantities.

The global *r.m.s* values are still very small (≤ 0.02 mag) as for infrared colors, while the maximum scatter (which occurs at the lowest temperatures and reflects a gravity dependence in the case of the (B–V) and a metallicity dependence in the case of the (V–I)) between the best fit and model atmospheres with selected metallicity or gravity is somewhat larger (~ 0.10 – 0.16 mag) than for the infrared colors.

A direct comparison between our color transformations in the (B–V) planes and those proposed by H95 using their Table 7 indicates an excellent agreement, with only a minor, systematic difference of 0.01 mag (our (B–V)–(F39W–F555W) are bluer than the corresponding H95 values).

In Fig. 14 we report the best model fits to the difference between the ground-based BC_V and BC_I and the corresponding WFPC2 BC_{F555W} and BC_{F814M} values, as a function of the (F439W–F555W) and (F555W–F814W) WFPC2 colors, respectively. As for the corresponding infrared quantities, cubic polynomial relations with very small scatters are required to transform the BC from the WFPC2 into the ground-based visual photometric system.

The numerical relations to transform the selected colors and BCs from the WFPC2 to the ground-based photometric system are listed below:

$$(B - V) = 0.024(F439W - F555W)^3 - 0.136(F439W - F555W)^2 + 1.060(F439W - F555W) - 0.014$$

$$(V - I) = 0.049(F555W - F814W)^3 - 0.077(F555W - F814W)^2 + 1.120(F555W - F814W) - 0.005$$

$$BC_V = BC_{F555W} + 0.016(F439W - F555W)^3 - 0.070(F439W - F555W)^2 + 2.092(F439W - F555W) - 0.001$$

$$BC_I = BC_{F814W} + 0.052(F555W - F814W)^3 - 0.110(F555W - F814W)^2 + 2.189(F555W - F814W) - 0.007$$

6. Conclusions

Using our synthesis code we derive homogeneous, self consistent color–temperature relations and BCs in the HST infrared and visual photometric systems.

We investigated the behavior of the derived quantities for different stellar parameters and adopted set of model atmospheres. Major results are:

- For a given set of model atmospheres, scatters larger than 0.01 mag in the inferred colors are only observed at low temperatures (≤ 6000 K) when models with different gravities and, to a lower degree, with different metallicities are compared.
- For given stellar parameters, the BCP98 and LCB97 sets of model atmospheres provide significantly different colors (up to a few tenths of a magnitudes) below 5000 K. The inferred discrepancies can be mainly ascribed to the corrections applied by LCB97 to the original grids of Kurucz’s model atmosphere spectra in order to match empirical color–temperature relations.
- The inferred BCs are less dependent on the adopted stellar parameters and model atmospheres than the colors, even at low temperatures.
- Very similar colors and BCs have been obtained for the different NICMOS and WFPC2 cameras.
- Average relations, with a negligible dependence on the stellar parameters and the selected NICMOS or WFPC2 cameras, can be adopted to provide useful transformations between the HST and ground–based photometric systems. In the low temperature domain the ground–based (B–V), (J–H) and (J–K) colors are bluer than the corresponding ones in the HST photometric system, while the ground–based (V–I) color is redder than the corresponding (F555W–F814W) one in the WFPC2 system.

We acknowledge Jon Holtzman for his careful Referee Report and comments and Laura Greggio for the helpful discussions and suggestions. We thank the STScI NICMOS Staff for providing the information on the NICMOS throughput curves. L.O. acknowledges the financial support of the “*Ministero della Università e della Ricerca Scientifica e Tecnologica*” (MURST) to the project *Stellar Evolution*.

REFERENCES

- Bessel, M. S., Castelli, F., & Plez, B. 1998, *A&A*, 333, 231 (BCP98)
- Castelli, F., 1997, private communication
- Holtzman, J. A., Burrows, J., Casertano, S., Hester J., Trauger, J. T., Watson, A. M., & Worthey, G. 1995, *PASP*, 107, 1065 (H95)
- Johnson, H. L. 1966, *ARA&A*, 4, 193
- Leitherer, C., & Heckman, T. M. 1995, *ApJS*, 96, 9
- Leitherer, C., et al. 1999, *ApJS*, in press
- Lejeune, T., Cuisinier, F., & Buser, R. 1997, *A&AS*, 125, 229 (LCB97)
- Montegriffo, P., Ferraro, F.R., Origlia, L., & Fusi Pecci, F. 1998, *MNRAS*, 297, 872
- Stephens, W., Frogel, J.A., Ortolani, S., Davies, R., Jablonka, P., & Renzini, A., 1999, *astro-ph/9909001*

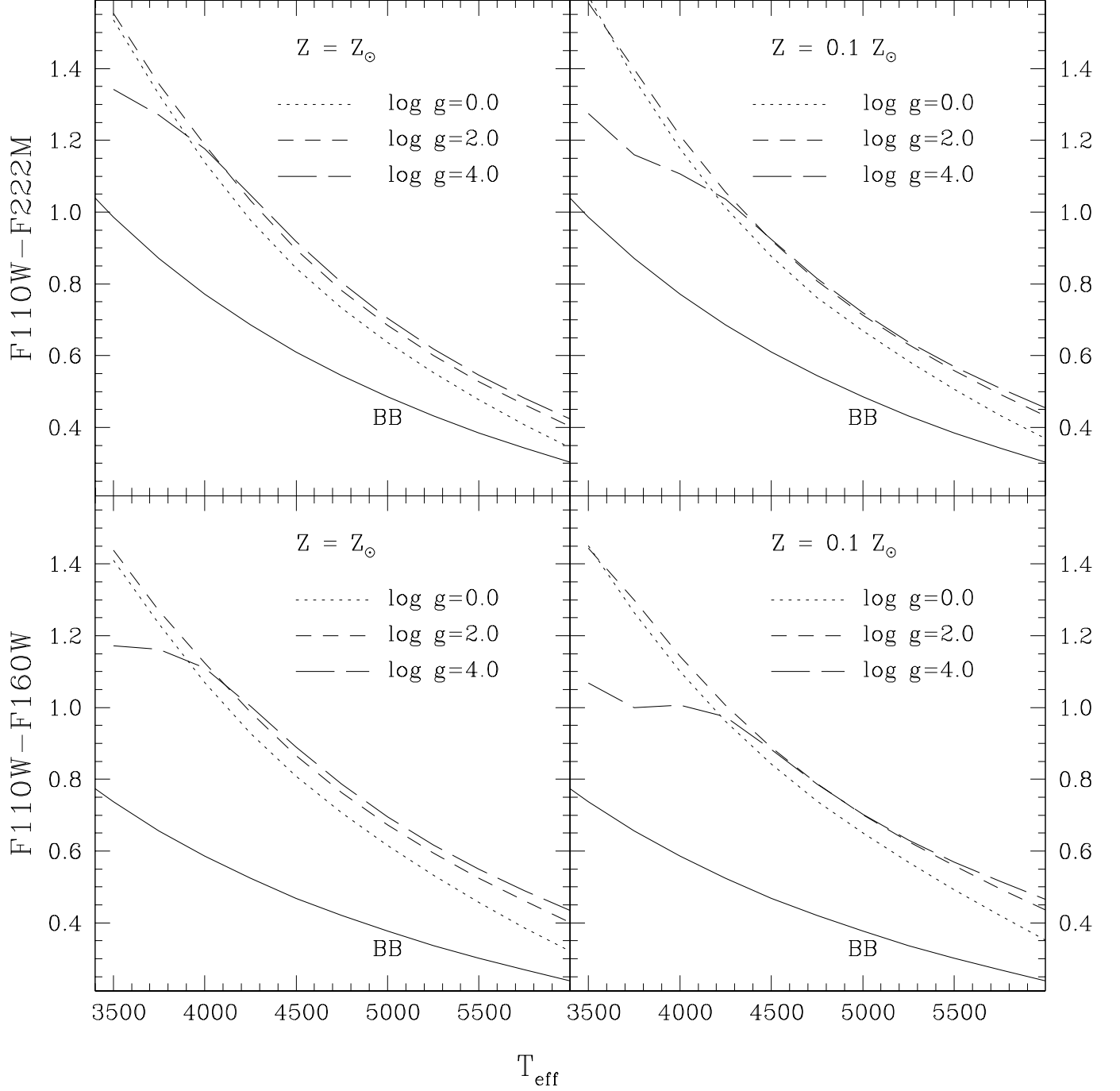


Fig. 1.— $(F110W-F160W)$ (bottom panels) and $(F110W-F222M)$ (top panels) color-temperature transformations in the HST-NIC2 system, using the BCP98 models. Relations using three different gravities ($\log g=0.0$: dotted line, $\log g=2.0$: short-dashed line; $\log g=4.0$: long-dashed line) and two metallicities ($Z = Z_{\odot}$ left panels, $Z = 0.1Z_{\odot}$ right panels) are shown. For comparison we also plot the relations for a pure blackbody (continuous line).

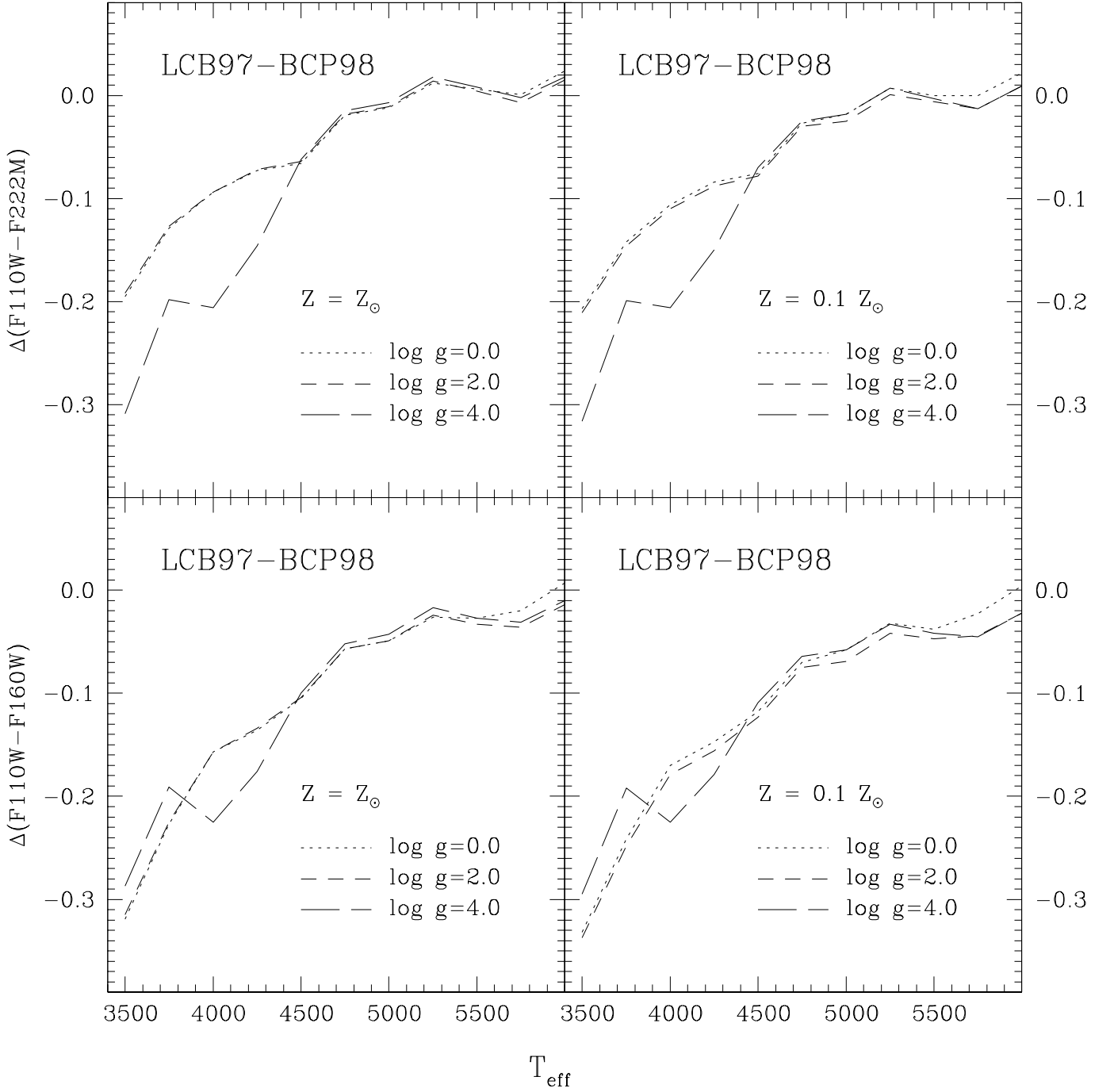


Fig. 2.— Differences of the color–temperature transformations in the NIC2 system, by adopting the BCP98 or the LCB97 model atmospheres. Notation as in Fig. 1.

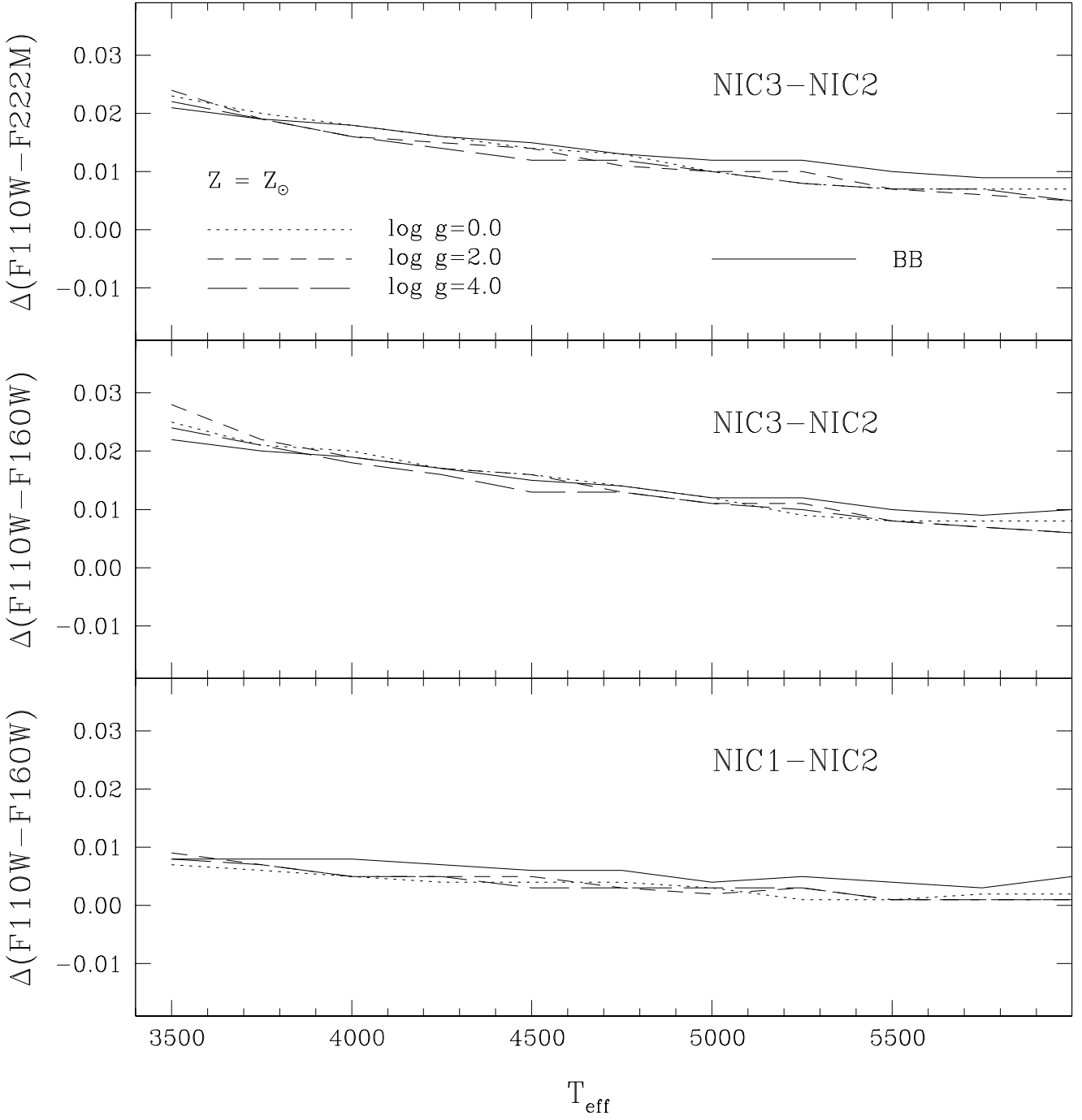


Fig. 3.— Differences of the (F110W–F160W) and (F110W–F222M) color–temperature transformations using the BCP98 models between the NIC2 and NIC1 or NIC3 systems at solar metallicity. Notation as in Fig. 1.

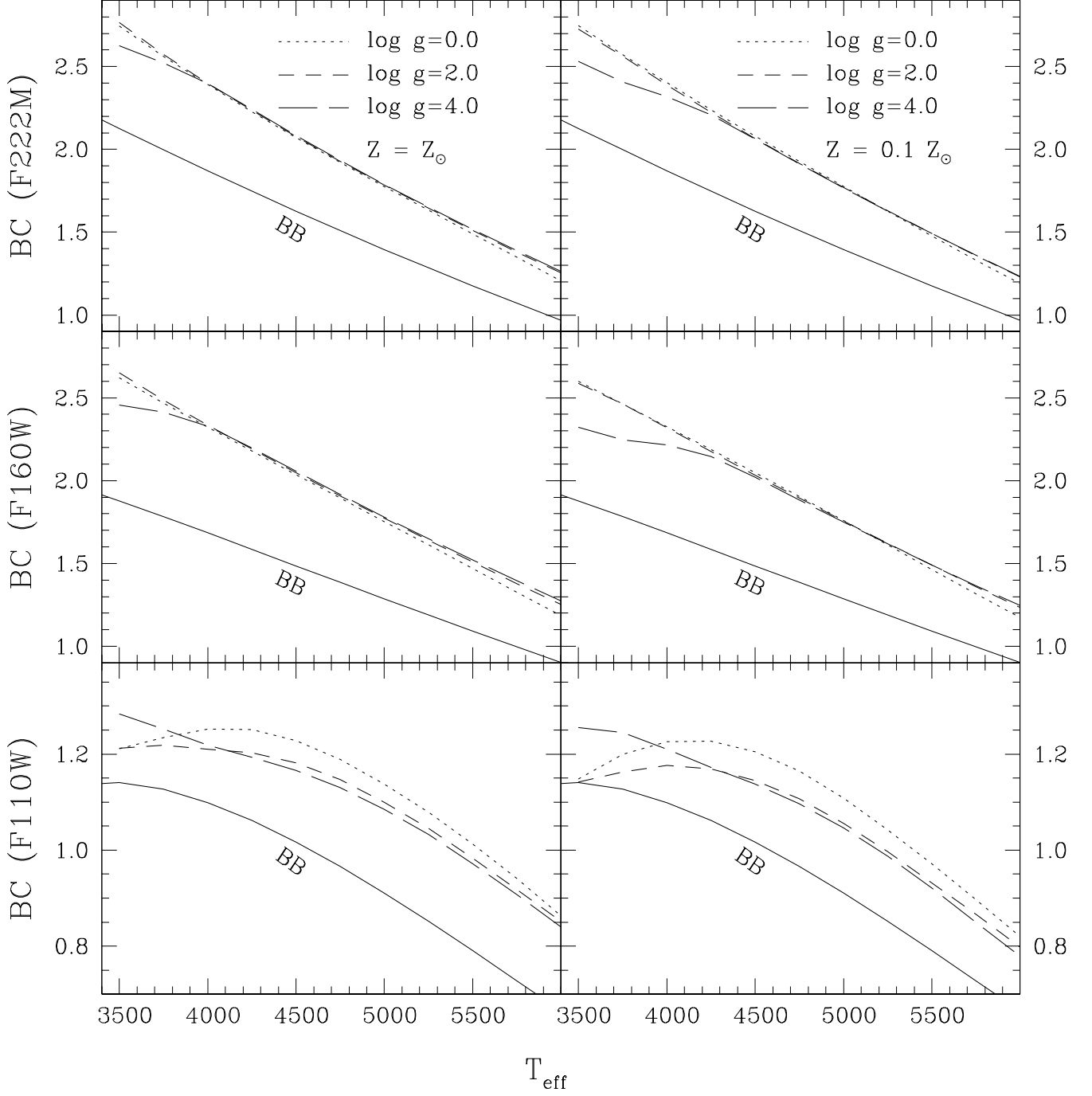


Fig. 4.— Bolometric corrections in the NIC2 F110W, F160W and F222M passbands as a function of temperature using the BCP98 models. Notation as in Fig. 1.

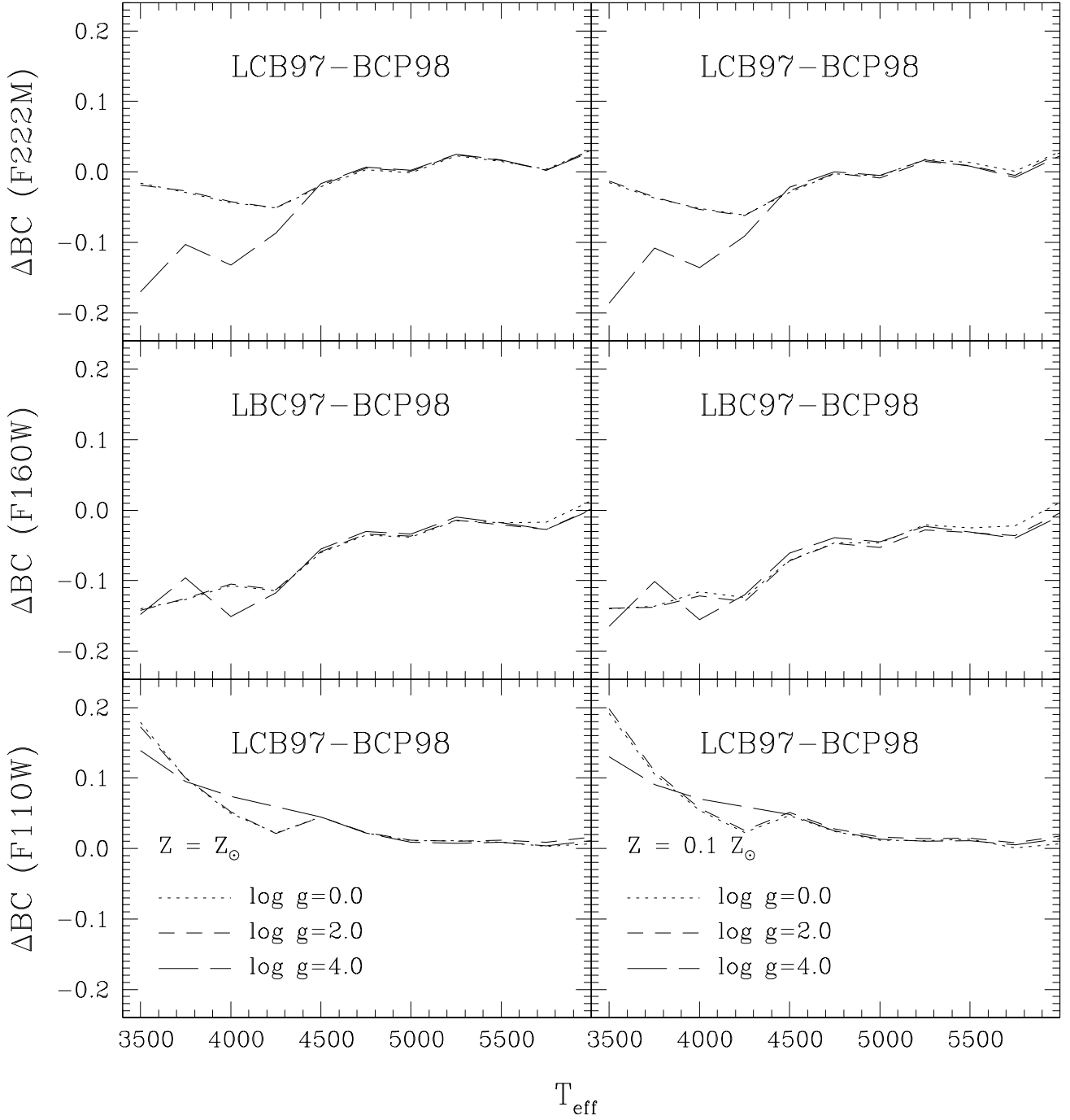


Fig. 5.— Differences between the values of the bolometric corrections in the NIC2 photometric system, adopting the BCP98 or the LCB97 models. Notation as in Fig. 1.

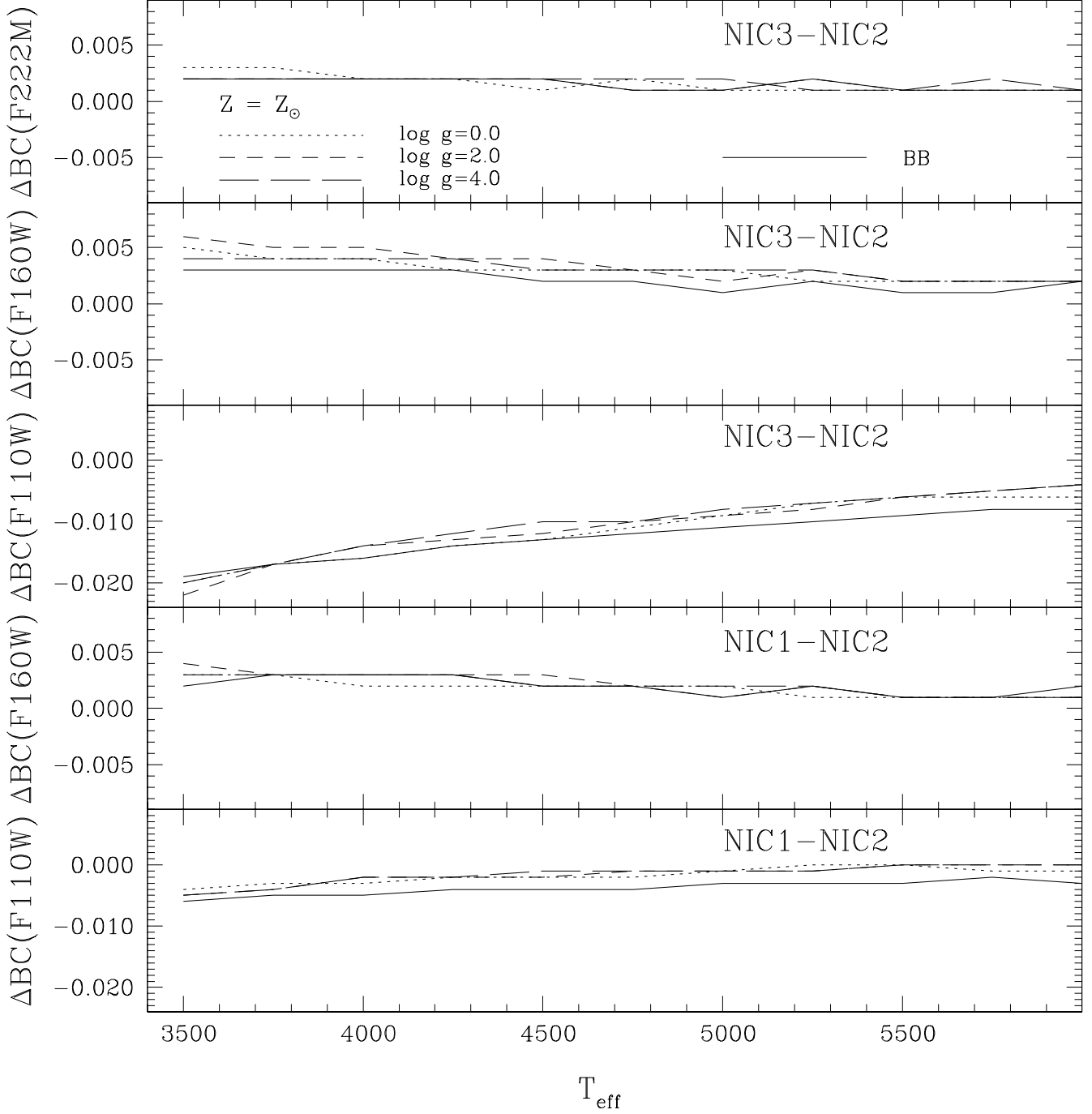


Fig. 6.— Differences of the F110W, F160W and F222M bolometric corrections using the BCP98 models between the NIC2 and NIC1 or NIC3 systems at solar metallicity. Notation as in Fig. 1.

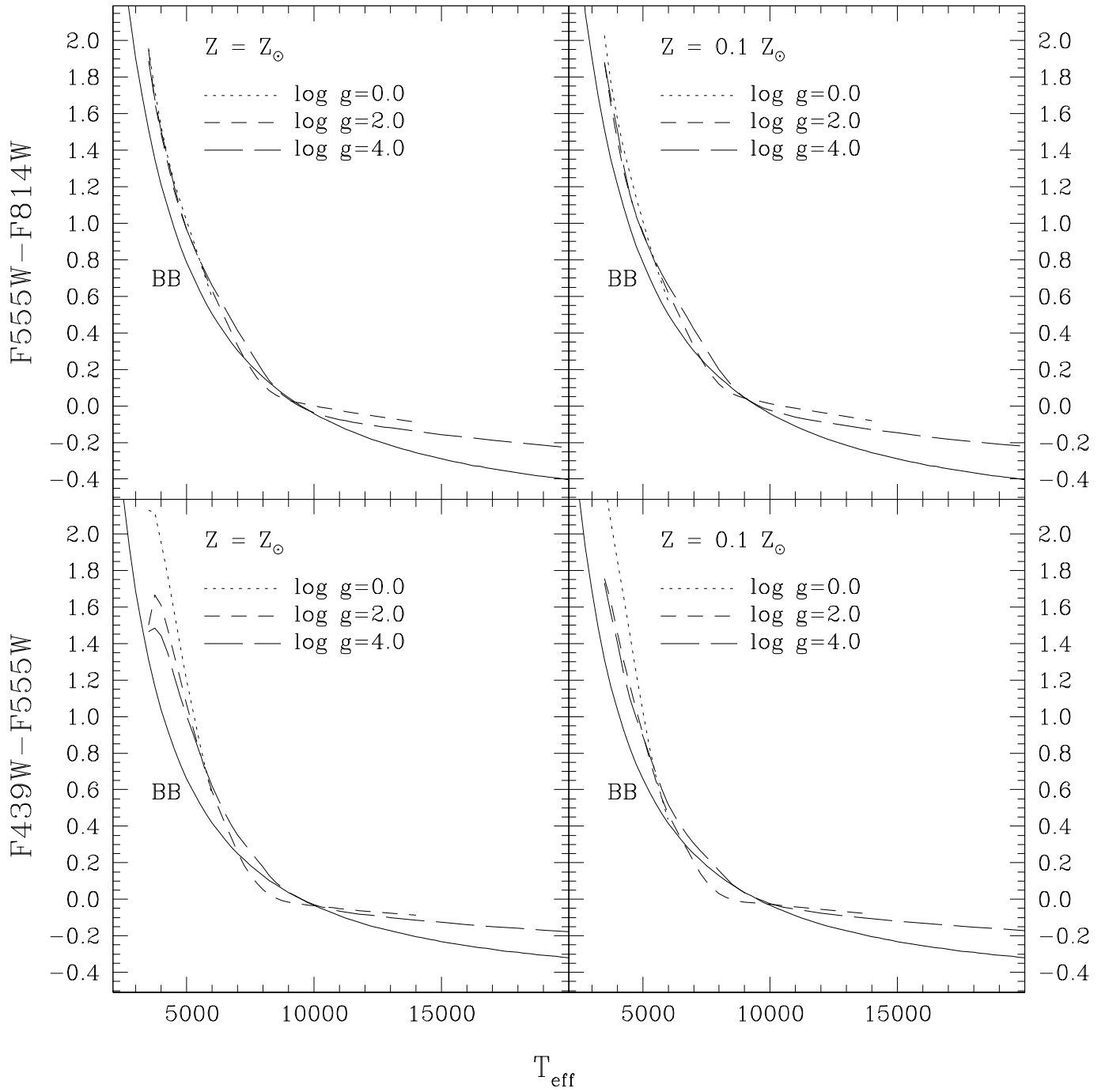


Fig. 7.— As in Fig. 1 but for the (F439W-F555W) and (F555W-F814W) colors in the PC1 system.

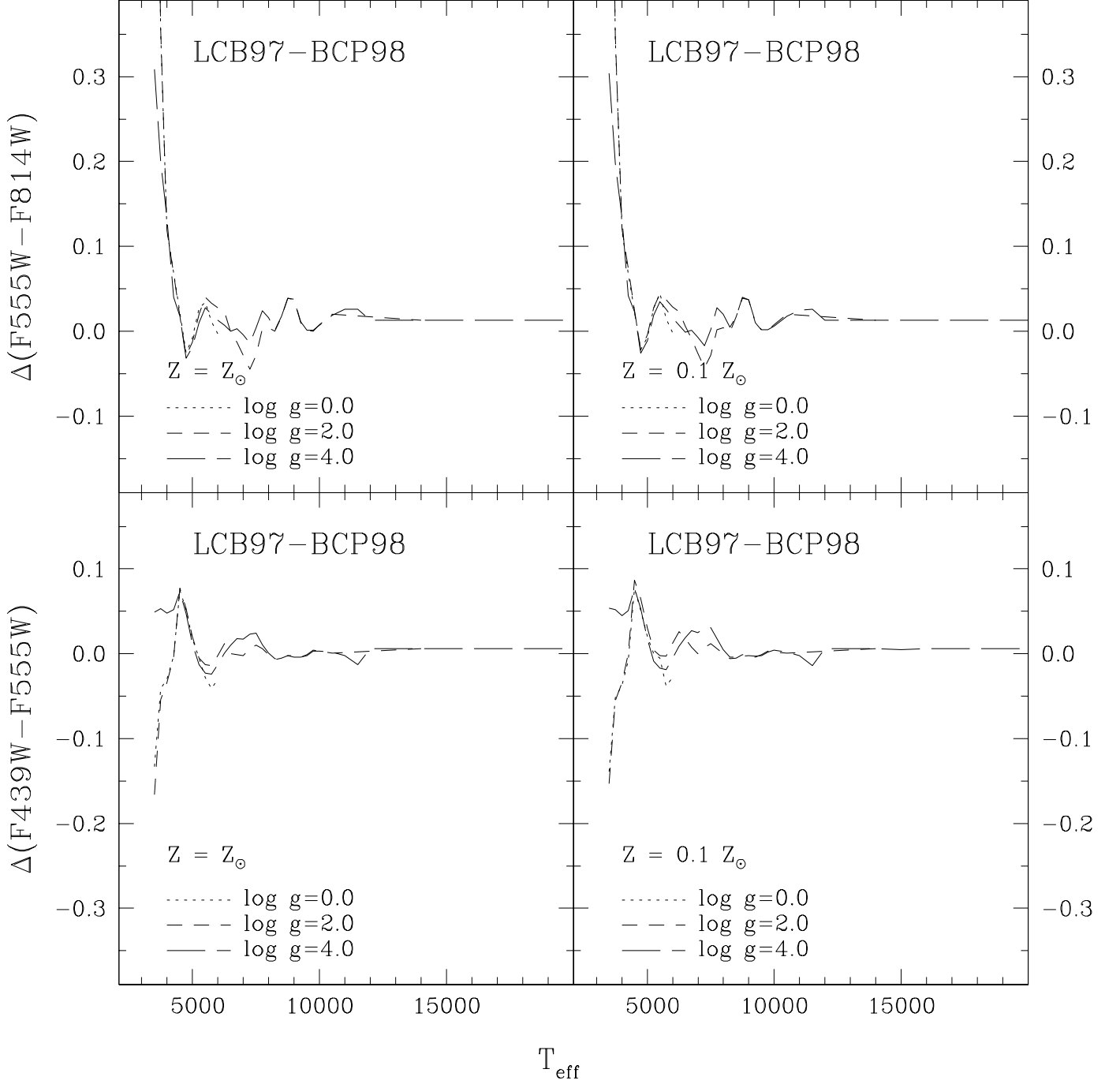


Fig. 8.— As in Fig. 2 but for the (F439W-F555W) and (F555W-F814W) colors in the PC1 system.

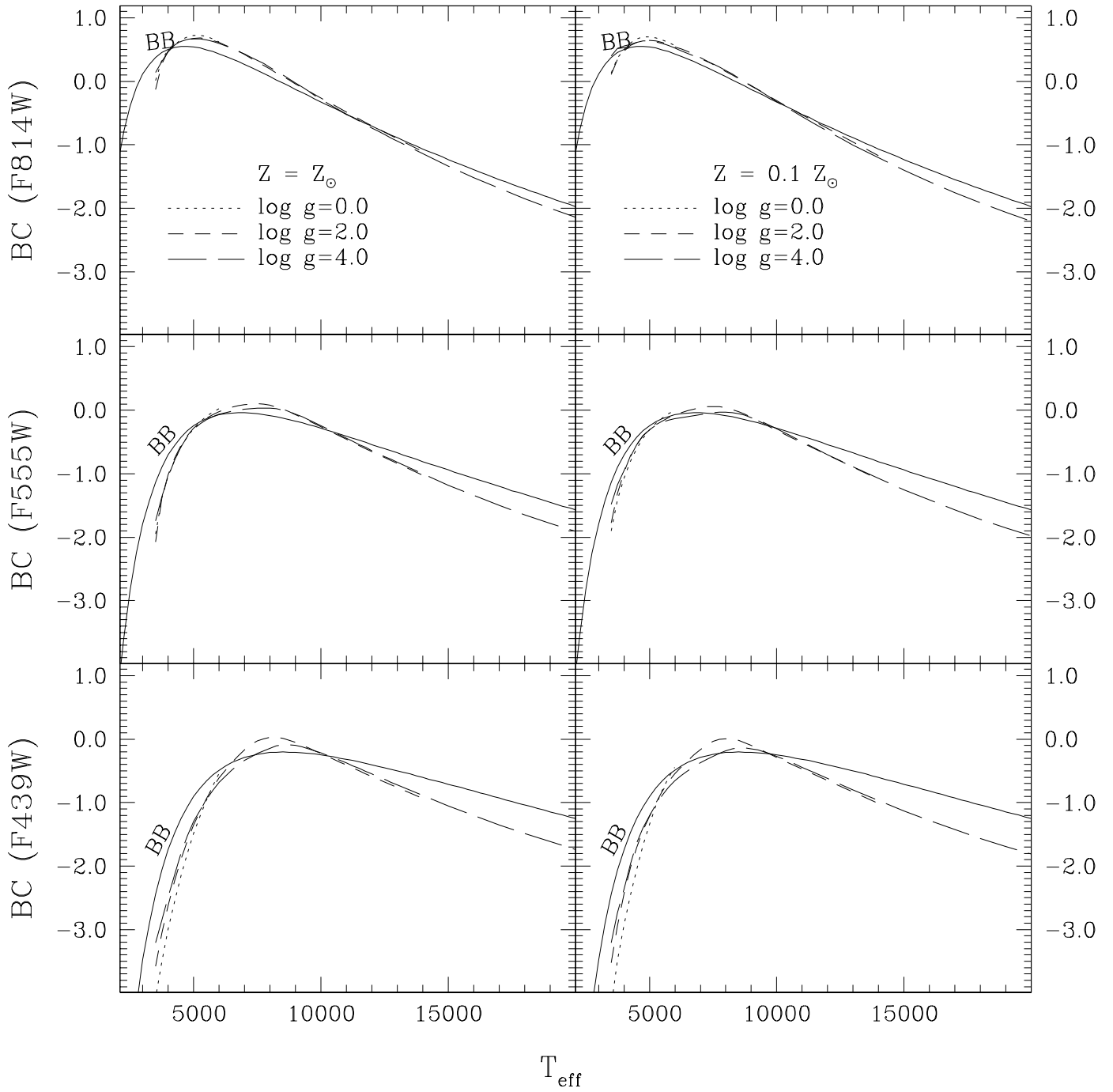


Fig. 9.— As in Fig. 4 but for the F439W, F555W and F814W bolometric corrections in the PC1 system.

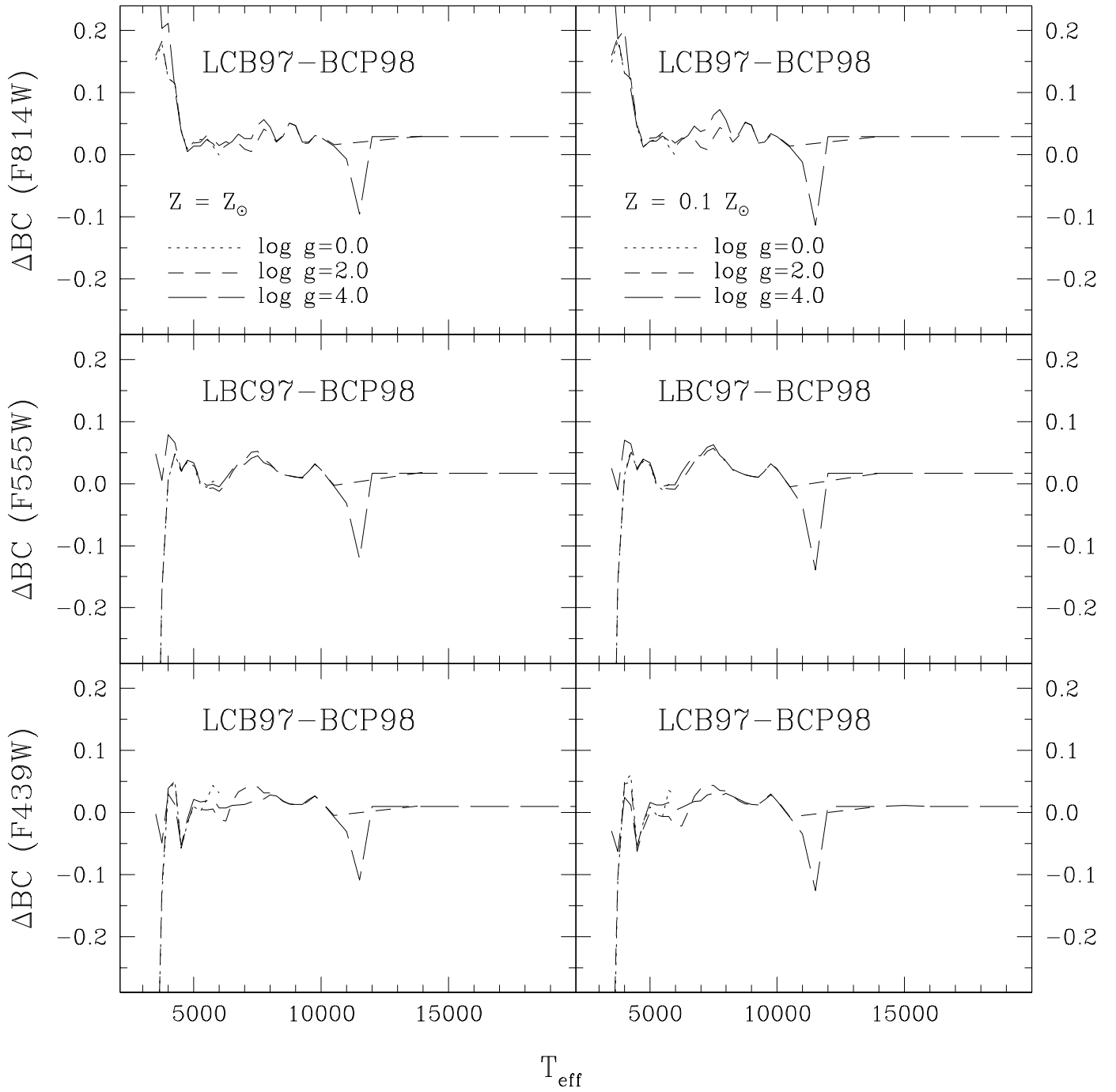


Fig. 10.— As in Fig. 5 but for the F439W, F555W and F814W bolometric corrections in the PC1 system.

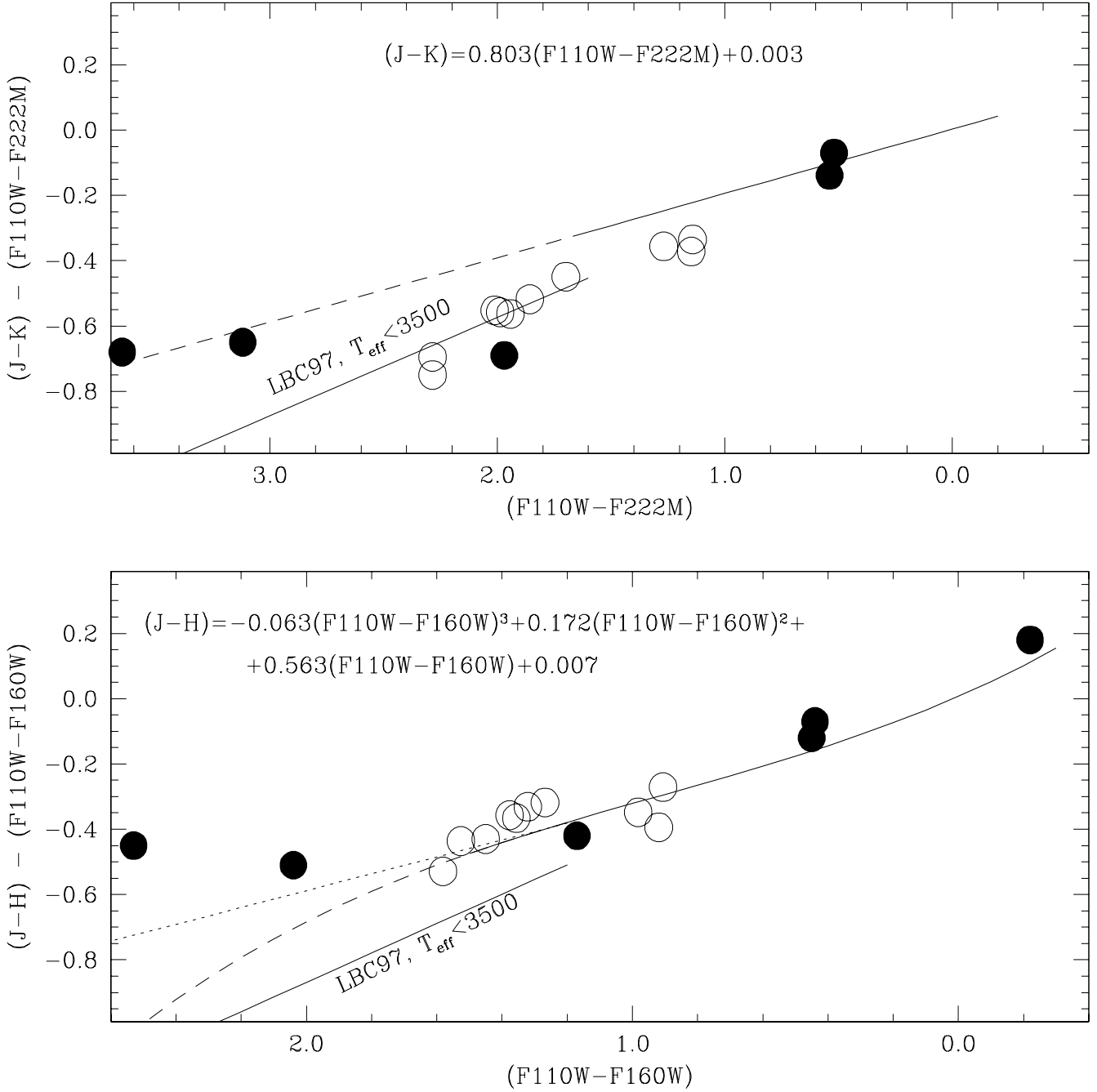


Fig. 11.— Model best fits to the difference between the $(J-H)$ and $(J-K)$ colors in the ground-based photometric system and the corresponding $(F110W-F160W)$ and $(F110W-F222M)$ values in the NICMOS system, as a function of the corresponding NICMOS quantities. Atmosphere: BCP98. Full circles are the observed values of the standard stars, according to the NICMOS Photometry Update WEB page. Empty circles refer to the set of red stars in the Baade's window measured by Stephens et al. (1999) with photometric errors ≤ 0.05 mag. Dotted and shaded lines are the linear and cubic extrapolated relations, respectively. For comparison, we also plotted the best fit using the LCB97 model atmospheres at temperatures below 3500 K.

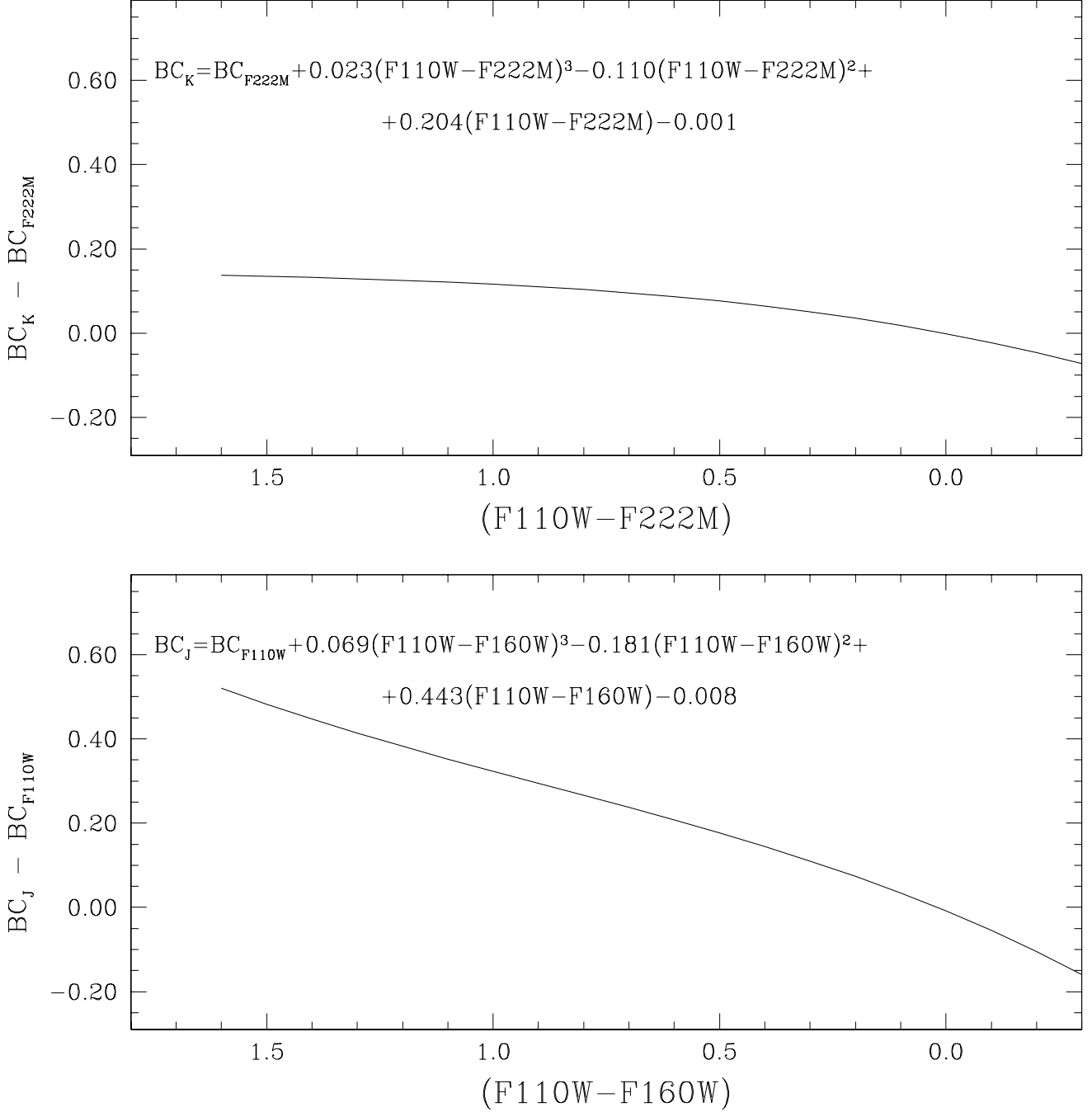


Fig. 12.— Model best fits to the difference between the BC_J and BC_K bolometric corrections in the ground-based photometric system and the corresponding BC_{F110W} and BC_{F222M} values in the NICMOS system, as a function of the $(F110W - F160W)$ and $(F110W - F222M)$ NICMOS colors, respectively. Atmosphere: BCP98.

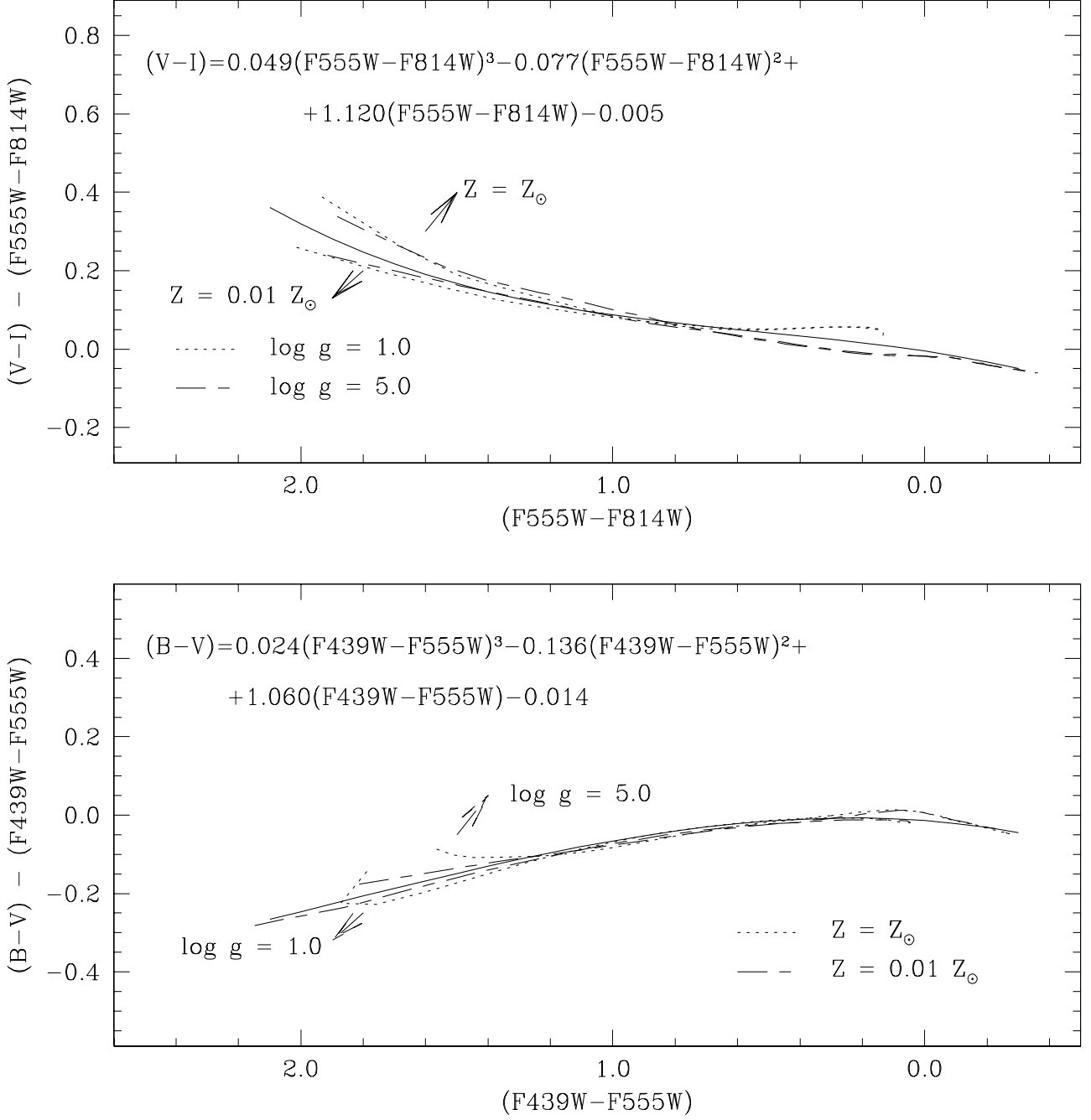


Fig. 13.— Model best fits to the difference between the (B-V) and (V-I) colors in the ground-based photometric system and the corresponding (F439W-F555W) and (F555W-F814W) values in the WFPC2 system, as a function of the corresponding NICMOS quantities. Atmosphere: BCP98. For comparison, together with the best fit we also plot the models at the two different gravities ($\log g=1.0$ and 5.0) and metallicities ($Z = Z_{\odot}$ and $Z = 0.01Z_{\odot}$).

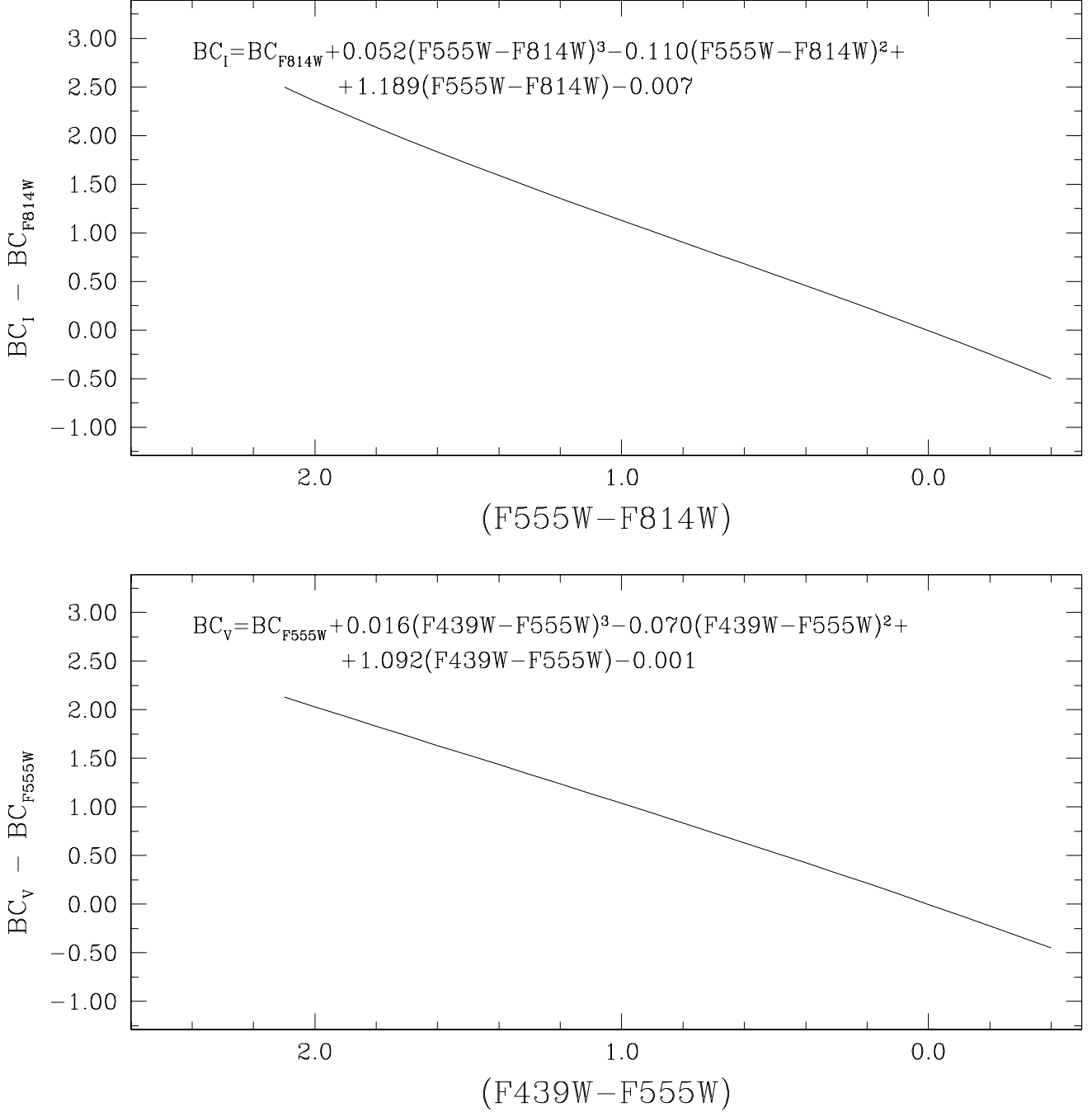


Fig. 14.— Model best fits to the difference between the BC_V and BC_I bolometric corrections in the ground-based photometric system and the corresponding BC_{F555W} and BC_{F814M} values in the HST system, as a function of the $(F439W - F555W)$ and $(F555W - F814W)$ WFPC2 colors, respectively. Atmosphere: BCP98.